Superconductor
Science and
Technology

PAPER • **OPEN ACCESS**

Impact of contact resistance on current distribution and performance of model CORC® cables with physical defects

To cite this article: V Phifer *et al* 2025 *Supercond. Sci. Technol.* **38** 085014

OPEN ACCESS
IOP Publishing
Superconductor Science and Technology
Supercond. Sci. Technol. **38** (2025) 085014 (16pp)
https://doi.org/10.1088/1361-6668/adf3e9

Impact of contact resistance on current distribution and performance of model CORC® cables with physical defects

V Phifer[1,2,3,*], L Cooley[2,3], D van der Laan[4,5] and J Weiss[4,5]

[1] VEIR Inc., Woburn, MA 01801, United States of America
[2] Florida State University, Tallahassee, FL 32306, United States of America
[3] National High Magnetic Field Laboratory, Tallahassee, FL 32310, United States of America
[4] Advanced Conductor Technologies, Boulder, CO 80301, United States of America
[5] University of Colorado, Boulder, CO 80309, United States of America

E-mail: phifer.va@gmail.com

Received 1 April 2025, revised 11 June 2025
Accepted for publication 24 July 2025
Published 19 August 2025

Abstract

This work investigates current redistribution around defects in conductor on round core (CORC®) cables. Special two tape CORC® cables were constructed containing just one tape per layer with a 100% I_c dropout in the outer conductor. Three different cable types were measured to investigate the impact of contact resistance between tapes, R_c, on current redistribution around local defects. An array of z-axis Hall sensors, which could be positioned at any location along the cable, monitored changes in the self-field due to current redistribution. A clear shift in Hall polarity occurs at the defect location, with Hall sensors producing a positive voltage upstream of the defect and a negative voltage downstream of the defect. As the current transfers around the defect, the 'good' tape is overloaded, initiating a normal zone. In cables with high R_c, voltage taps reveal that the normal zone is confined to the 'good' tape, while the 'bad' tape remains superconducting. This normal zone can remain stable even at currents above I_c and can cause significant power dissipation, 590 mW at 60 A. As R_c decreases, facilitating better current sharing, the normal zone spreads to both tapes. These experiments have demonstrated that R_c can have a significant impact on power dissipation and that current sharing is essential for robust cable performance.

Keywords: current distribution, CORC, contact resistance, REBCO, current sharing, HTS cables, superconductivity

* Author to whom any correspondence should be addressed.

1. Introduction

$REBa_2Cu_3O_{7-\delta}$ (REBCO, RE = rare earth) coated conductors are at the forefront of high temperature superconductor applications. Their ability to retain high current densities in large magnetic fields coupled with their large tensile strength makes them a promising conductor for applications such as high field magnets, electric machines, fusion energy, and power transmission [1]. Unfortunately, the tape conductor manufacturing process can result in lengthwise variations in the tape critical current, I_c, sometimes resulting in significant dropouts [2–4]. These variations are often localized and can be due to a variety of factors both intrinsic, e.g. related to variations in flux pinning, grain misalignment, second phases and variations in composition, etc [2, 5, 6], and extrinsic, e.g. related to slitting cracks and variation in conductor dimensions, etc [2, 7]. Providing alternative current paths reduces the risk of hotspot formation by permitting current to redistribute around tape I_c dropouts. One option for promoting current sharing is to use multi-conductor cables.

This study focuses on conductor on round core (CORC®) cables and wires, manufactured by Advanced Conductor Technologies (ACT). CORC® is composed of multiple layers of REBCO tapes, helically wound around a copper former, resulting in a flexible cable architecture [8]. There is presently strong interest in CORC® cables for high-field magnet applications due to macroscopically isotropic properties and winding configurations like those for round wires [9, 10]. A cable's current sharing capability is intimately coupled to the tape-to-tape contact resistance, R_c, which depends both on intrinsic factors such as the electrical resistivity of the materials making the contact and extrinsic factors such as the presence of corrosion, the contact topography, external transverse pressure, and so on. The contacts between tapes in CORC® are limited to periodic crossovers instead of continuous overlap, which can result in both large overall R_c and variable R_c values for each crossover as discussed in [11]. The topography of the contacts at these crossovers may be the most important factor in determining R_c. Mechanical tape slitting can deform the Hastelloy layer, producing a 4–10 μm hook at the tape edge. This hooked edge confines most of the tape-to-tape contact to the perimeter of the crossovers, utilizing perhaps 10% of the available contact area [11]. Coating the tapes in PbSn solder fills in topographical disparities, resulting in a smoother surface and more uniform contact. Winding cables from PbSn coated tapes reduced R_c by 4 orders of magnitude when compared to regular REBCO tapes. Heating the cables with PbSn-coated tapes produced further reduction of overall R_c and its variability, where microstructural analyses showed that practically all of the available contact area was utilized [11].

The magnet group at Lawrence Berkeley National Laboratory (LBNL) has investigated Hall sensors as a quench detection method [12–14]. Hall sensors detect changes in the current distribution due to normal zone generation and can be more sensitive than traditional voltage taps. In CORC®, current flows along the conductors in a solenoidal path as indicated by the black and gray arrows in figure 1(a). The adjacent layers are wound in opposing directions, i.e. clockwise versus counterclockwise, such that the axial field components cancel out when the current is uniformly distributed between conductors. Gaps between crossovers allow radial magnetic field to extend outward from the cable axis, with the magnitude of field varying periodically along the cable axis, figure 1(b). The z-axis Hall sensors will detect a periodic signal in accordance with the field orientation reflected in figure 1(b). The presence of a defect causes current redistribution between tapes, producing imbalance in the field components which can be detected by z-axis Hall sensors. Figure 1(c) plots a representative magnetic field distribution due to current redistribution. The LBNL group has shown that current redistribution occurs mainly at the terminations in cables with a large R_c [14].

Taken together, the surface condition of contacts, the limited number of contacts along the cable length, the presence of extrinsic factors, especially hooked copper at tape edges, and the high variability of R_c from contact to contact suggest that current sharing in CORC® may be much more difficult to assess than has been previously acknowledged. The majority of current sharing studies in REBCO cables have been based on simulations [15–19], where details of contacts were set up from inadequate or incomplete information. By contrast, here we report an experimental investigation into current sharing around significant I_c dropouts. In this work we used an array of Hall sensors to investigate changes in the current distribution along cables containing physical defects. We also look into the possibility of using scanning Hall sensors as a non-invasive method for determining the location of defects in cables [20].

2. Cable geometry and experiment setup

Based on the results of the R_c study in [11], we examined three different cable types specially constructed for us by ACT to probe the impact of R_c on current sharing in CORC® cables. The three different cables are:

1. Cu cable: wound from 2 mm SuperPower tapes with 5 μm electroplated Cu on a 30 μm Hastelloy substrate.
2. PbSn cable: wound from 2 mm SuperPower tapes with 5 μm electroplated Cu on a 30 μm Hastelloy substrate and coated in PbSn solder
3. Soldered cable: the PbSn cable after undergoing a heat treatment of 5 min at 200 °C to melt the solder

To simplify the geometry and minimize possible current redistribution pathways each cable contained only 2 layers, with 1 REBCO tape per layer (I_c = 49 A), figure 2(a). The inner tape is referred to as Tape 1, while the outer tape, which contains a defect, is referred to as Tape 2. Each cable was 50 cm in length with the defect located at 25 cm. The defect was created by tearing the outer tape as shown in figure 2(b). In addition to the above cable types, we also measured two Baseline cables which did not contain any known defects. Both cables were wound from untinned REBCO conductors. The ends of the cable were unwound as detailed in [11] permitting

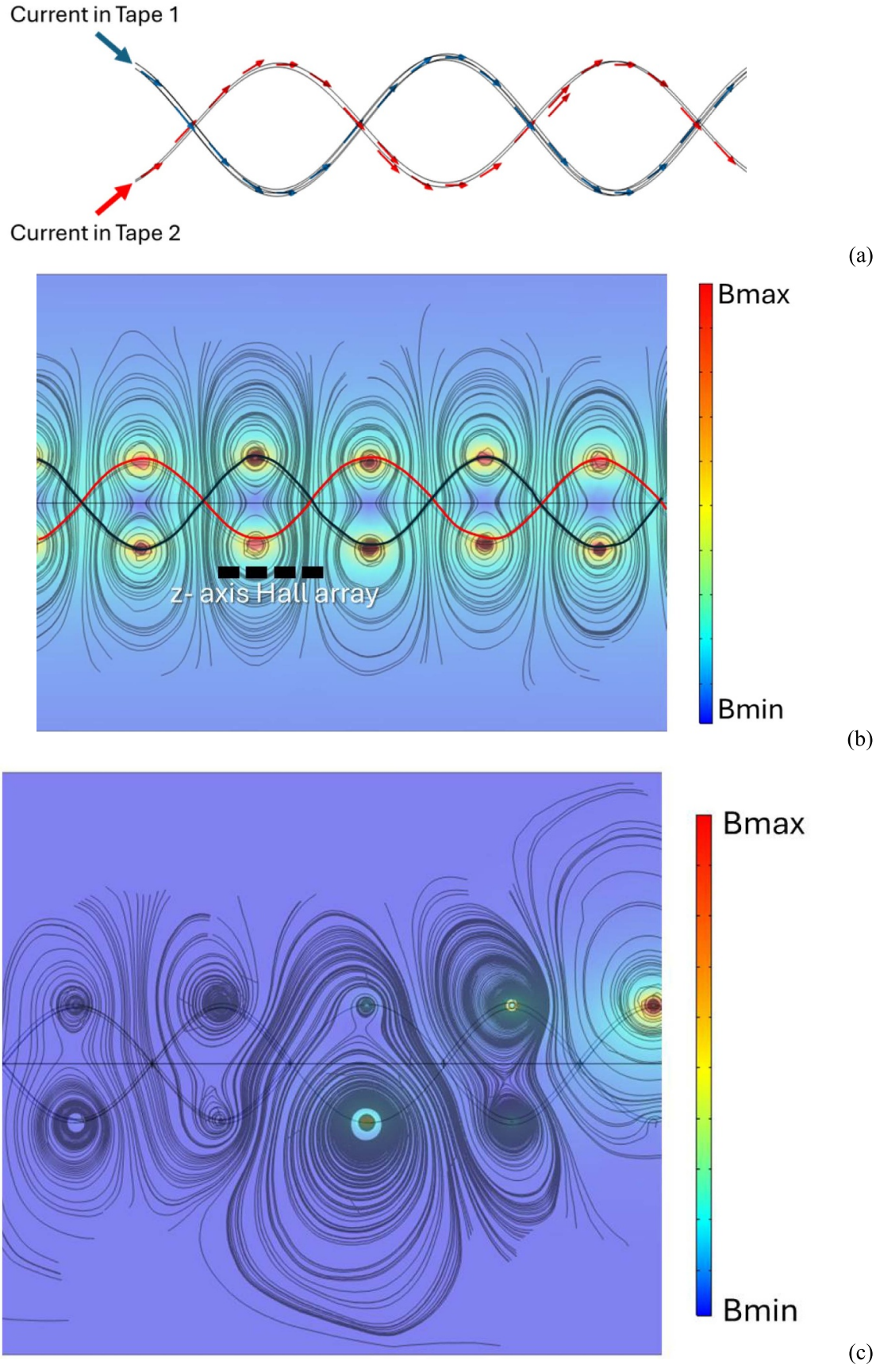

Figure 1. (a) Current path in two helically wrapped tapes in the cable, (b) and resulting magnetic field in the two tape CORC® cables with streamlines highlighting regions along the cable with field parallel to the Hall sensors and regions perpendicular to the Hall sensors, (c) representation of imbalance in magnetic field due to current redistribution around a defect.

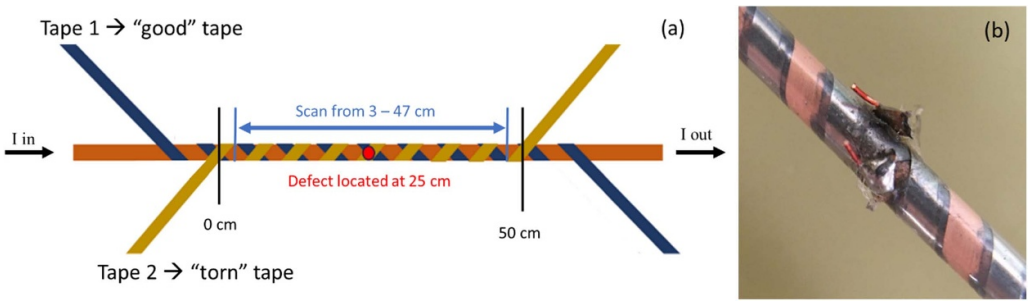

Figure 2. (a) Geometry of two tape cables measured with a defect located in the center of the outer tape, (b) defect created by tearing the tape.

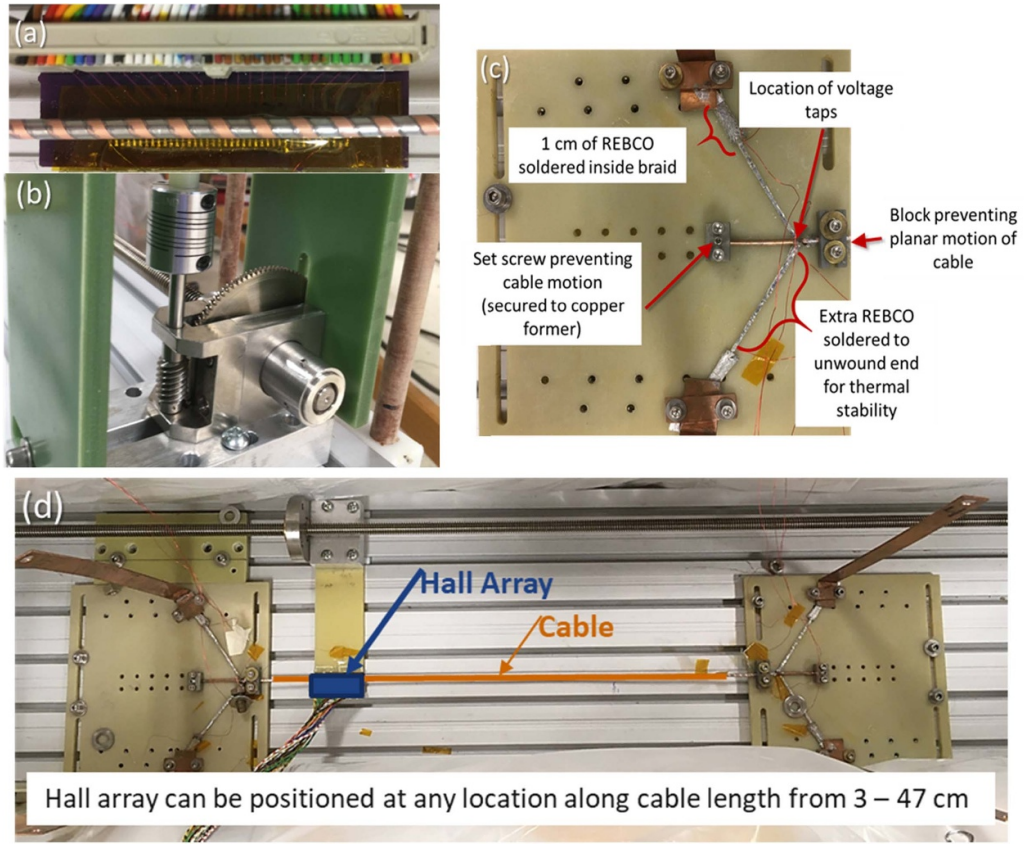

Figure 3. (a) Hall sensors located underneath cable, (b) worm gear which moves array along cable, (c) cable and Hall array setup, (d) overhead view of entire setup.

the tapes to be energized independently. Only 1 conductor was energized in the measurements of Baseline 1 while in Baseline 2 both conductors were energized.

Current redistribution was measured, in a bath of liquid nitrogen, LN_2, and at self-field, using a Hall array of 18 GaAs z-axis Hall sensors, located directly underneath the cable, figure 3(a). In this position the Hall sensors measure changes in the radial magnetic field produced by current transfer. The position of the Hall array is controlled by a stepper motor connected to a worm gear and lead screw, figure 3(b), and can be positioned at any location along the cable axis. Figure 3(d) shows an overhead view of the entire setup, in which the right end of the cable was firmly secured to the aluminum back plate, while the left end of the cable was loosely secured, allowing for difference in thermal contraction between the back plate and the cable. Due to the hardware securing the cable, the Hall sensors were unable to measure the 3 cm of cable on either end. Therefore lengthwise scans were from 3 to 47 cm. The measurements consisted of recording the Hall sensor voltage (in response to the cable self-field) as the cable current was ramped to a maximum current (dependent on conductor I_c values), held for 3 s, and ramped down. Then the Hall array was moved along the cable and the measurements were repeated.

The traditional ACT terminations were not used in these measurements, instead each tape received its own termination connected to a shunt resistor to measure the current flowing into and out of each tape. This setup allowed us to measure current sharing in situations of uneven current injection,

i.e. current injected into 1 tape but extracted from both. It was necessary to provide both mechanical and thermal stability to the unwound tape ends as any movement or overheating could damage the REBCO layer. Each end of the cable was secured at two points to prevent any rotational or planar motion. The unwound tapes were mechanically stabilized by applying a set screw in the Cu former and securing the cable in a channel as detailed in figure 3(c). When investigating current sharing it is necessary to drive current above I_c which generates voltage to redistribute current around normal zones. Since there is only 5 μm of Cu stabilizer on the REBCO tapes, the unwound ends are exceptionally vulnerable to burnout at just a few amperes above I_c. Therefore, a segment of 2 mm REBCO was soldered to the unwound ends for added thermal stability.

3. Interpretation of hall data for baseline cable

3.1. Understanding the periodic hall response along the length of a cable

The general response of the Hall sensors during a stationary current ramp is depicted in figure 4. In the ideal case, where there are no defects in either conductor, the Hall sensors produce a linear increase/decrease in voltage in response to a linear current ramp with no change in voltage when the current is held steady. Different ramp rates showed no significant changes in the linearity of the Hall response. A small magnetization effect in the Hall sensors is noted by the spread in base values after the initial ramp, but it was not affected by differing ramp rates. The Hall sensors used for these measurements were uncalibrated having different offsets. In addition the sensors were hand soldered leading to slight variations in sensor orientation. These two factors could influence the 16% variation in Hall voltages as seen when holding the current steady.

The Hall response is fairly uniform along a cable in the absence of any current sharing. The Hall voltages along Baseline 1, carrying 10 A, are plotted in figure 5. Each dot in figure 5(b) represents the voltage produced by a Hall sensor, while holding current as shown in figure 5(a), at that location along the cable, with each color corresponding to a different sensor. Note that this tape had degraded, such that its I_c was only 15 A (normally $I_c \sim 70$ A for 2 mm tapes), thus lengthwise measurements were confined to 10 A for this sample. The range in signals is on the order of 150 μV and the lengthwise mean is 90 μV. The 150 μV spread in signals is due to the location of the Hall sensors with respect to the tape face. As depicted in figure 1(b), the cable geometry results in radial field leakage leading to a periodic Hall response. This periodicity becomes evident when considering a single 3 cm section measured by the array for Baseline 2, figure 6(a). For this particular measurement the current was ramped to 60 A, so the magnitude of the Hall sensors is larger than those in figure 5, however the spread, 110 μV, is in line with measurements for Baseline 1. Plotting only the voltages that are centered on a tape face we see the spread collapse, figure 6(b). The periodicity of Hall voltage with respect to location along cable is clearly depicted in figure 6(c) which plots the signal from a single Hall sensor as it scans along the cable axis. Here we see the Hall voltage, depending on its location, ranges between -20 and 160 μV. These plots highlight that, in the absence of current sharing, the Hall sensors produce a $\sim$150 μV periodic spread in signals due to the location of the Hall sensors with respect to tape location. Note that if these measurements were performed on a higher I_c conductor the magnitude of the Hall signals would be expect to increase, but the overall pattern would persist.

3.2. Response in baseline cables without defects

Figure 7 plots the Hall response along the length of Baseline 2, with the inset cartoon showing the direction of current flow. The current was ramped to a maximum of 75 A. For the first 30 cm of the cable's length the spread in Hall signals is approximately 150 μV, corresponding to the spread measured in Baseline 1, and is due to the location of the sensors with respect to the conductors. In the absence of current redistribution, these regions are interpreted as having current flowing mainly in the individual conductors.

As the current nears the negative terminations the spread in Hall voltages increases by a factor of 2–5, this increased spread in Hall signals is interpreted as regions with increased current transfer. Current redistribution in a cable without any known defects is due to an imbalance in the termination resistances, R_t. Shunt resistors were connected at each end of the two tapes with the goal of measuring the current into and out of each tape. Unfortunately the resistance in the shunts, which is several orders of magnitude larger than the superconductor and inter-tape contact resistances, ends up dominating the circuit voltages. A small imbalance in terminal resistances, R_t, ends up driving the current distribution and forcing the current to transfer. The setup detailed in figure 3 makes it quite difficult to achieve uniform resistances at the current contacts. Instead of a single contact point, as in a cable termination, each unwound end has both a soldered contact and a press contact, resulting in more opportunities for disparity in resistances to arise. A large difference in the resistance of the current leads (1.4 mΩ vs 2.4 mΩ) into each tape resulted in 70% of the current being injected into Tape 1 and only 30% into Tape 2. However, on the other end of the cable R_t is nearly identical between tapes (1.5 and 1.7 mΩ), thus to balance the voltages current is forced to transfer from Tape 1 into Tape 2, which is detected by the Hall sensors. Figure 8(a) plots the current injected into and extracted from each tape against the total cable current.

When the current direction is reversed, we see the same spread in Hall signals, figure 8(a), confirming that the spread is not due to sensor degradation or localized cable effects. In this case the current splits evenly between the two tapes, but there is an imbalance in the negative terminations, forcing the

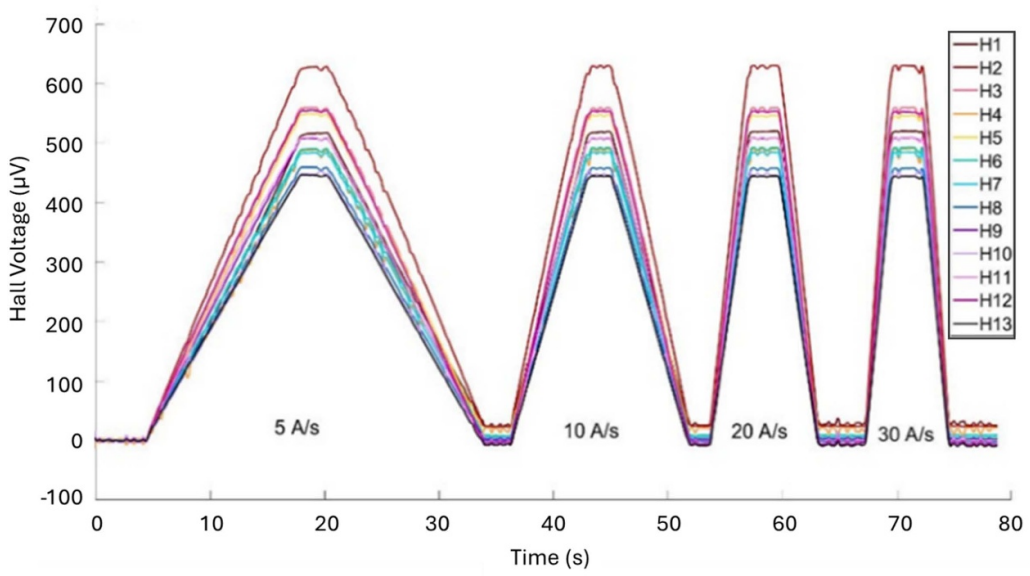

Figure 4. General Hall response of Baseline cables showing no significant impact from using different ramp rates.

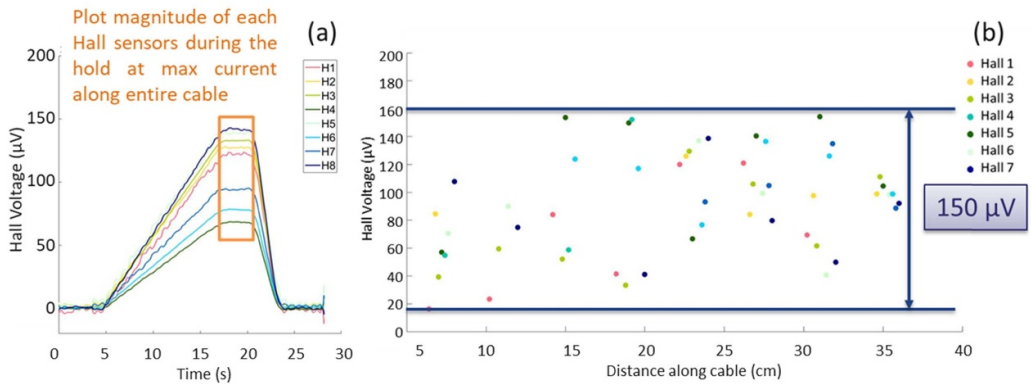

Figure 5. (a) Hall ramp highlighting data from the holding period, which is averaged, (b) Hall response along length of a Baseline 1 carrying 10 A.

current to transfer out of Tape 2. The current imbalance for the reversed polarity is plotted in figure 8(b).

3.3. Forced current transfer

The Hall response along the cable when current is forced to transfer (current injected into one tape and extracted from the other) is quite similar to those for cable Baseline 2. Figure 9 plots the Hall voltages produced along the length of the Cu cable for 20 A of current transfer. No current transfer occurs along the first two-thirds, interpreted from the 150 μV spread in Hall signals. Between 30 and 40 cm we see a sixfold increase in the spread of the Hall voltages, suggesting that most of the current transfer occurs in this region. Instead of uniform current transfer along the entire cable, we see a reluctance to transfer current, with most of the redistribution occurring near at 30–40 cm. This corresponds to the current transfer length of the cable defined in [11]as $L = \sqrt{\frac{I_{tr} R_c p}{2 A_x N_{tape} E_c}}$ by, where A_x is the crossover area, I_{tr} is the current transferred, p is the pitch, N_{tapes} is the number of tapes current is transferring into, and E_c is the electric field criterion. For an $R_c \sim 500$ $\mu\Omega{\cdot}cm^2$ the expected current transfer length would be approximately 30 cm.

4. Results

4.1. Cu cable with 100% tear in Tape 2

The Cu cable had a relatively large R_c of 500 $\mu\Omega$ cm^2, which is approximately half the average value found for the control cables [11]. This decrease is likely due to a change in lubrication, which ACT implemented after the completion of the R_c study. The Hall voltage produced while holding current at 68 A is plotted along the cable length in figure 10. A clear shift in the polarity of the Hall sensors occurs at the defect. Upstream of the defect, current transfers out of Tape 2 and into Tape 1

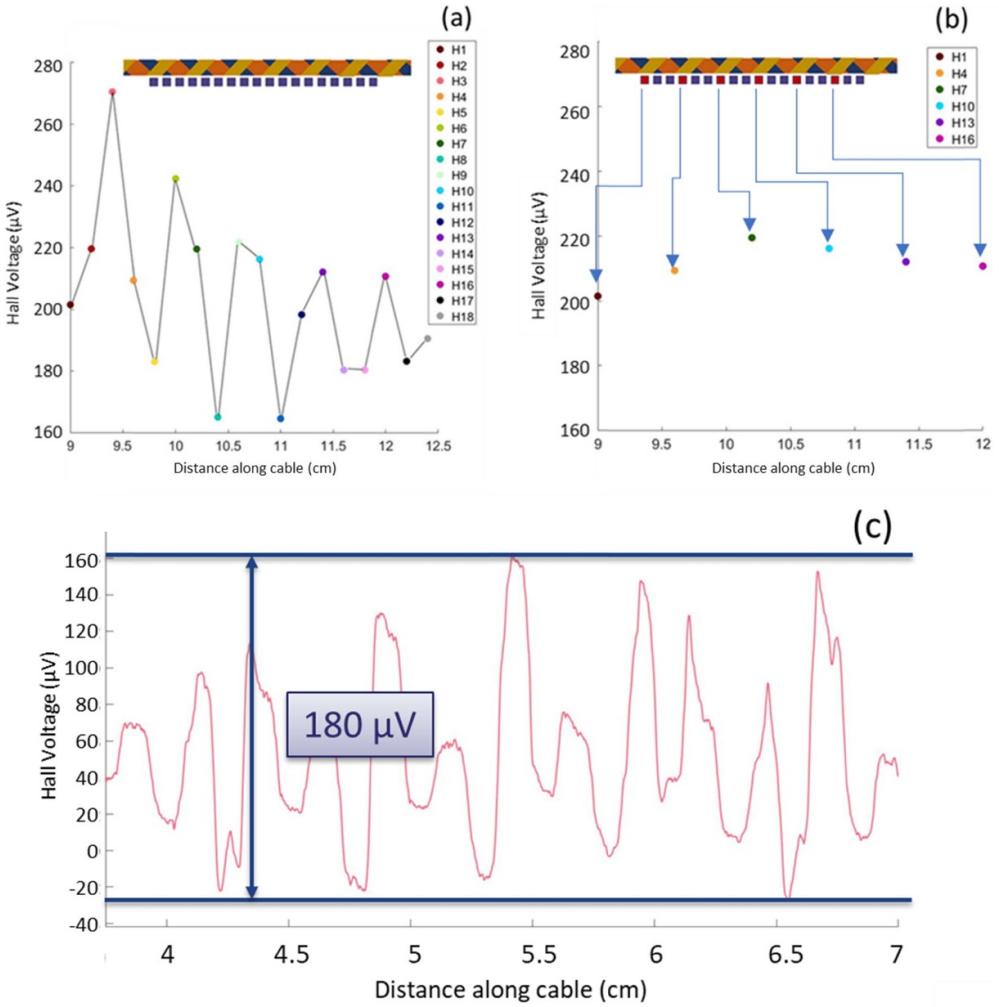

Figure 6. (a) Periodic signal from Hall array, (b) signal from only those sensors which are centered on a tape face, (c) scan of a single sensor along cable showing periodic response.

producing a positive Hall voltage. Downstream of the defect, current transfers back into Tape 1 producing a negative Hall voltage. Figure 11 shows what the Hall response looks like over the entire measurement cycle upstream and downstream of the defect.

Upstream of the defect the spread in signals is 300 μV, approximately double the baseline spread, suggesting a small amount of current sharing. The spread increases to 600 μV in the 5 cm region just upstream of the defect, implicating a reluctance to redistribute the majority of current until necessary. Downstream the range in Hall voltages is only 200 μV, in this region the majority of the current is either in Tape 1 or in the copper core. There is a significant increase in current transfer occurring in the last 10 cm of the cable indicated by a 1000 μV spread in Hall voltages. The large R_c results in poor current sharing as it appears that the current prefers to remain in the good tape and only transfers back to balance the termination voltages. Based on our interpretation of the Hall data, a simple circuit depicting the uneven current flow in the Cu cable, the double arrows representing the current imbalance, is shown in figure 12. The high R_c delays current transfer downstream of the defect until the termination is encountered.

The schematic in figure 13 outlines all the voltage taps monitoring the system. Unwinding the ends of the cable also allowed us to apply numerous voltage taps to monitor the voltage buildup in each tape as well as the voltage produced from current transfer. Figure 14 plots the corresponding voltages against the cable current. Examining the cable voltages gives some insight into the current transfer patterns in the cable. There are 4 main takeways from figure 14.

1. *The normal zone is confined to Tape 1.* The solid red line plots the voltage across Tape 1, the good tape, which begins to transition around 35 A. It is possible that Tape 1 was damaged during the process of creating a defect in Tape 2, degrading I_c by 15 A. The voltages in Tape 2 upstream (diamonds) and downstream (circles) of the defect are zero and show no signs of transition. Note that the dashed line labeled Tape 2 in figure 14 was produced by a voltage tap located on either end of the 'bad' tape. Since this tape had a

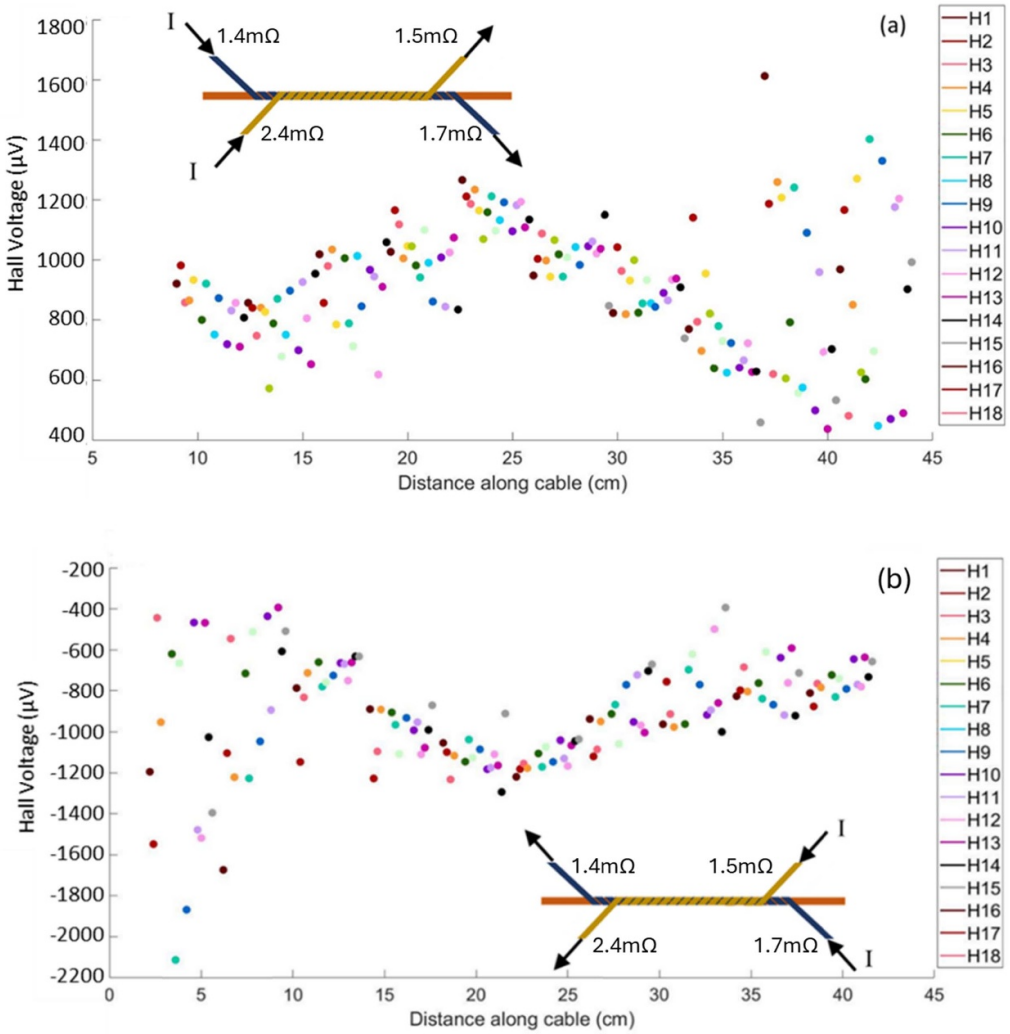

Figure 7. (a) Hall voltages along the length of cable Baseline 2, (b) with reversed current direction.

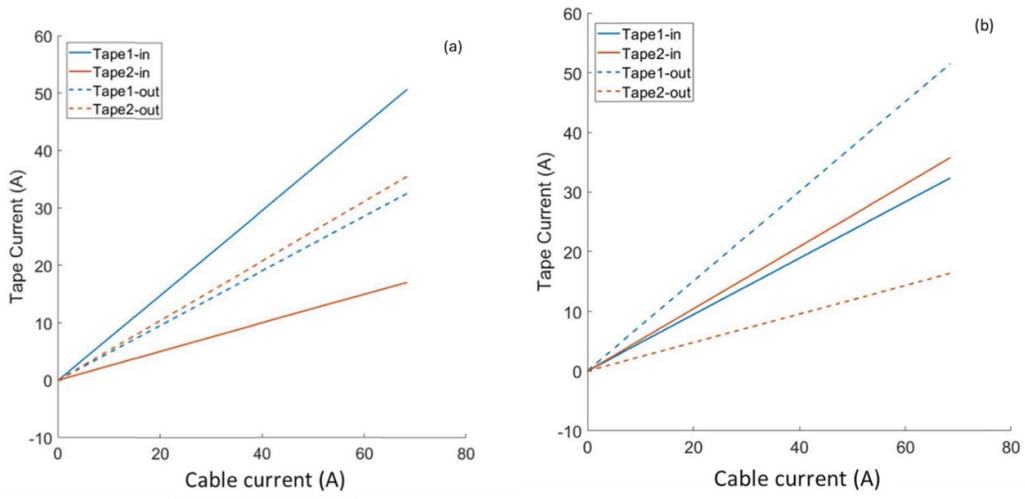

Figure 8. (a) Current distribution at the terminations, (b) current distribution at the terminations with reversed current polarity.

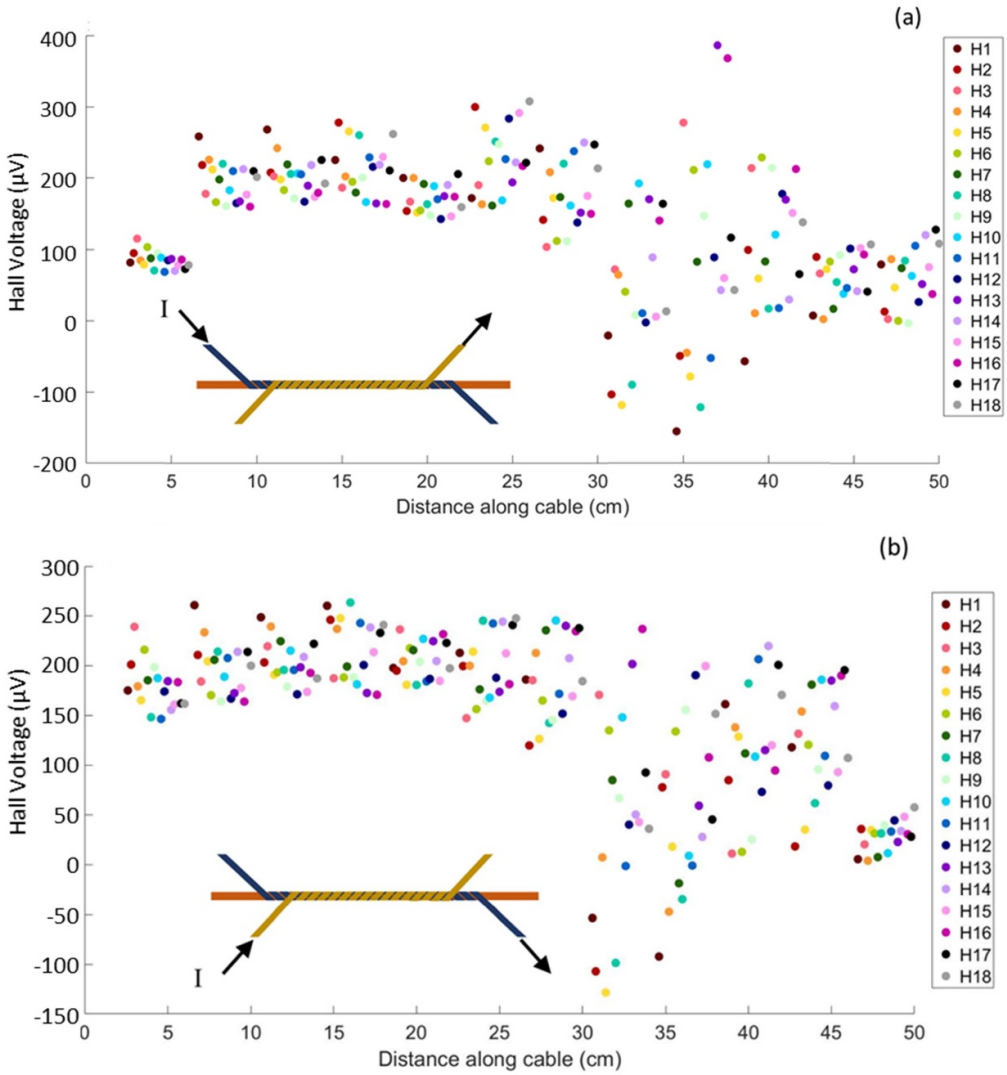

Figure 9. Forced current transfer from (a) Tape 1 to Tape 2 and (b) Tape 2 to Tape 1.

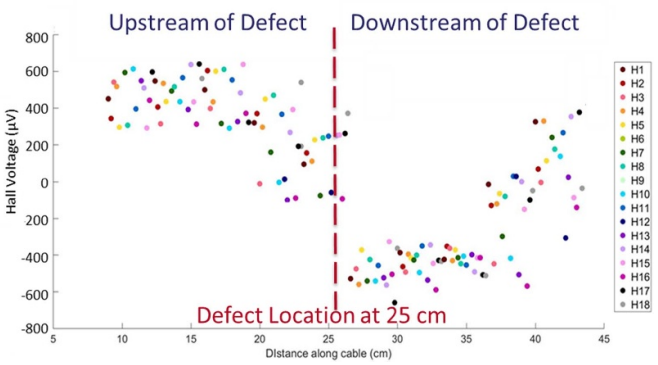

Figure 10. Plot of the Hall voltage at 68 A along the Cu cable shows a clear shift from positive to negative at the defect location.

100% I_c dropout the voltage measured is the summation of all current transferring out of the tape upstream and back into the tape downstream. As all the current injected into Tape 2 transfers into Tape 1 it forces a transition in the 'good' tape at the defect location. While we see no transition upstream and downstream of the defect we do begin to see a transition in the Tape 2 voltage tap. This transition occurs between the two voltage taps located on either side of the defect. Since there is a discontinuity in this transition is not due to the defect, but rather it is likely due to the good tape heating up locally, lowering I_c of the bad tape on either side of the defect.

2. *The normal zone is upstream of defect*. As Tape 1 transitions, the voltage produced by current transfer upstream of the defect (x's) becomes nonlinear, while voltage from current transfer downstream (triangles) remains linear. Therefore the normal zone which is likely located at the defect is spreading upstream of the defect rather than uniformly in both directions.
3. *Voltages from current transfer are larger than the voltage in Tape 1*. This might explain why the current does not transfer until necessary.
4. *When the cable current is below the I_c of Tape 1, all current transferring from Tape 2 to Tape 1 occurs upstream*

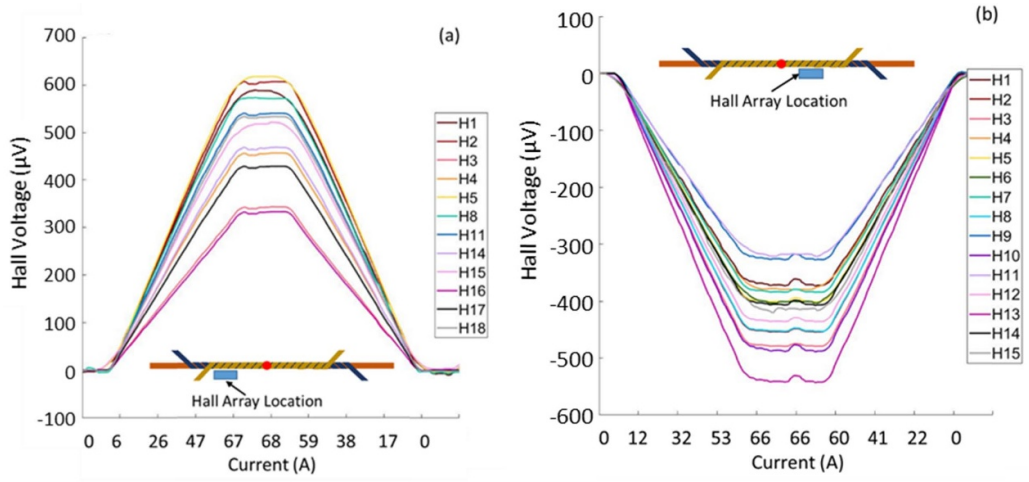

Figure 11. Hall response plotted against current (a) upstream of the defect, (b) downstream of defect (See Appendix A for plots along the entire cable length).

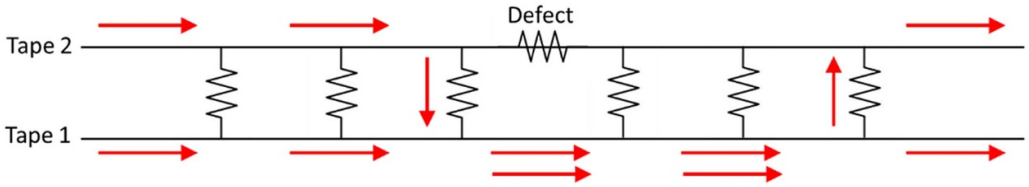

Figure 12. Simple circuit diagram showing interpreted current flow in Cu cable.

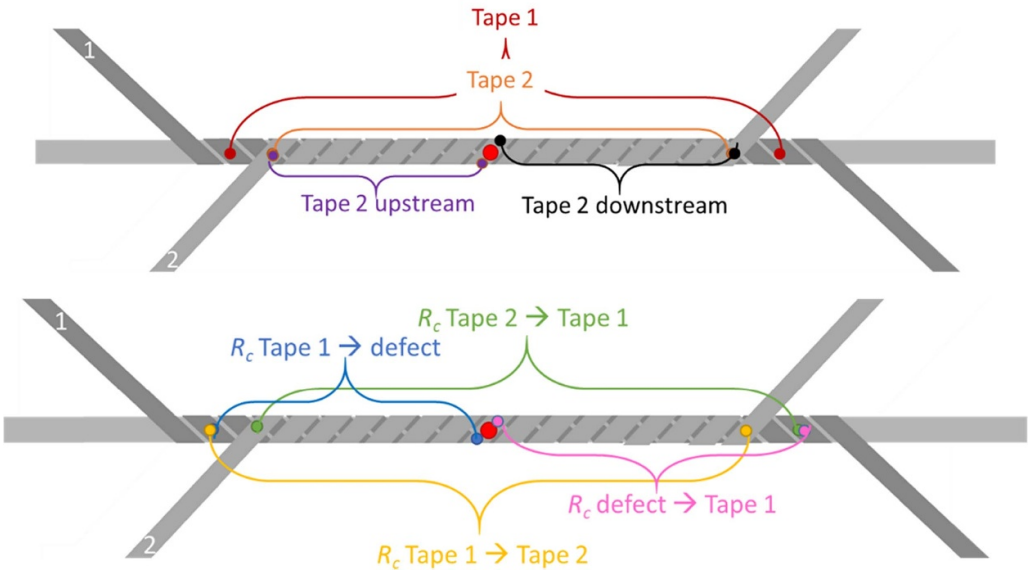

Figure 13. Cartoon showing all the voltage taps used to monitor the cable.

of the defect, while all current transferring from Tape 1 to Tape 2 occurs downstream of the defect. The plots of transfer voltage upstream of the defect (x's) and of transfer voltage from Tape 2 to Tape 1 (squares) over the entire cable are identical until a cable current of 50 A. Since these two voltages are equivalent we can conclude that all current transferring from Tape 2 to Tape 1 occurs upstream of the defect. If current was transferred downstream of the defect it would be reflected by a difference in voltage. Similarly, the plots of transfer voltage downstream of the defect (triangles) and of transfer voltage from Tape 1 to Tape 2 (sideways triangles) over the entire cable are identical until a cable current of 35 A.

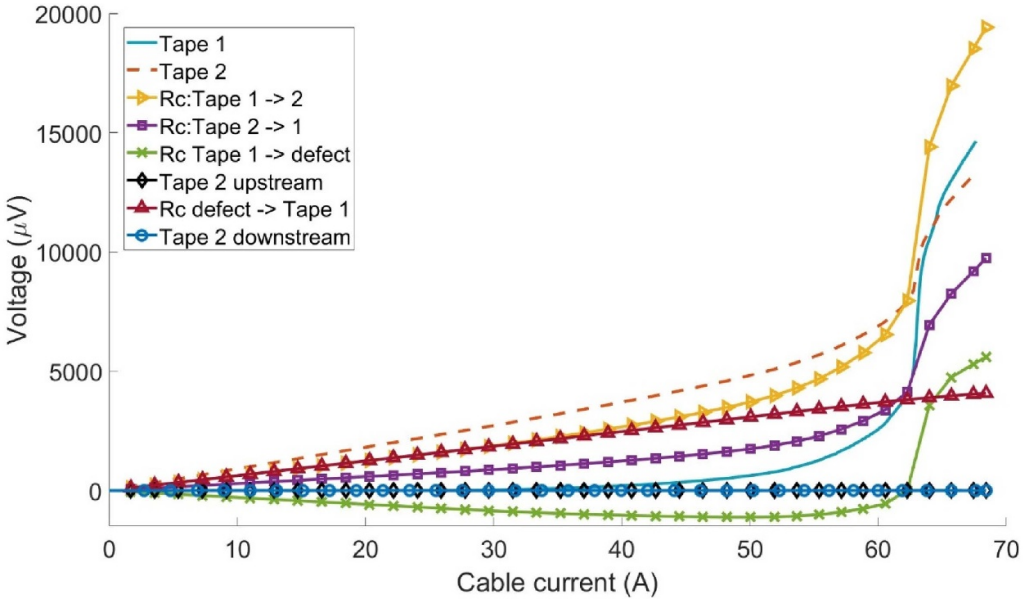

Figure 14. Voltages in the Cu cable.

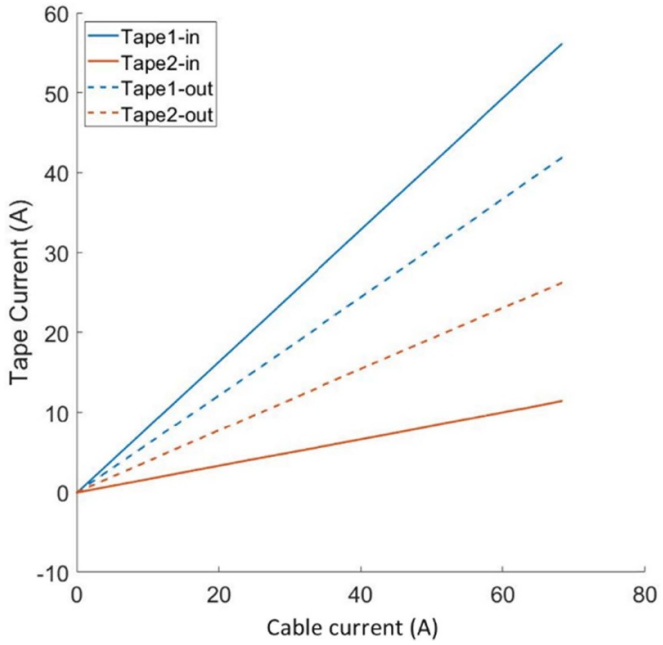

Figure 15. Current distribution in the Cu Cable.

One thing to note is that current distribution in this cable is not even, plotted in figure 15. As previously mentioned, large and unbalanced R_t drives the distribution between tapes. However, the presence of a complete dropout may further impact distribution as only 11 A out of 68 A is injected into Tape 2.

4.2. PbSn cable with 100% tear in Tape 2

The Hall response along the length of the PbSn cable was similar to the Cu cable. Upstream of the defect the Hall response is mainly positive, while downstream the response is mostly negative, but near the defect we see a cinching of the Hall signals, figure 16. In contrast to the Cu cable, the lower R_c was reduced to 11 $\mu\Omega$ cm^2, which facilitates better current sharing as indicated by the much larger spread in Hall signals, $\sim$ 1200 μV, upstream and downstream of the defect. The spread in Hall voltages over the 10 cm region near the defect is $\sim$ 150 μV, suggesting that near the defect no current transfer occurs and the majority of the current is flowing along the cable axis, either in Tape 1 or the copper former (see figure 1(c)). Figure 17 shows what the Hall response looks like over the entire measurement cycle upstream and downstream of the defect. Figure 18 shows a simple circuit diagram with our interpretation of the likely current paths in the PbSn cable.

The voltages in the PbSn cable, figure 19, are very similar to those in the Cu cable except that they are an order of magnitude smaller. Again, we see that the normal zone is limited to Tape 1 (solid line) with no indication of Tape 2 transitioning upstream (diamonds) or downstream (circles) of the tear. Note the voltage in Tape 2 (dashed line) measures the voltage across the defect, which captures the summation of all the current transferring into and out of the tape as well. Again we see Tape 2 begin to transition, this transition is confined to the region near the defect. The voltages from current transfer upstream (x's) and downstream (triangles) of the defect do not seem to be impacted by Tape 1's transition. This suggests a stable normal zone with no propagation at the defect. When the cable current is below the I_c of Tape 1, all current transferring from Tape 2 to Tape 1 occurs upstream of the defect, while all current transferring from Tape 1 to Tape 2 occurs downstream of the defect. However, above I_c the normal zone may cause more dynamic current redistribution.

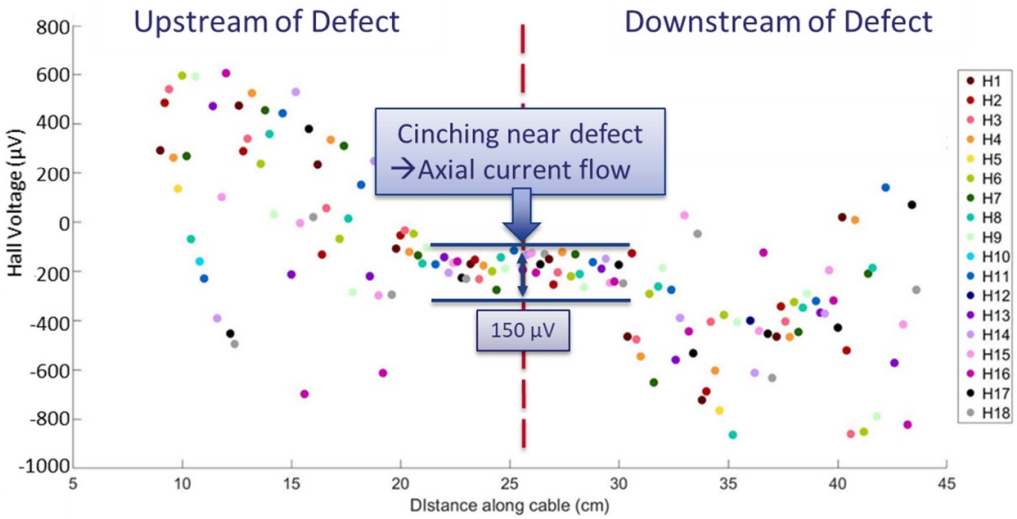

Figure 16. Plot of the Hall voltage along the PbSn cable shows a shift from positive to negative with 'cinching' at the defect location.

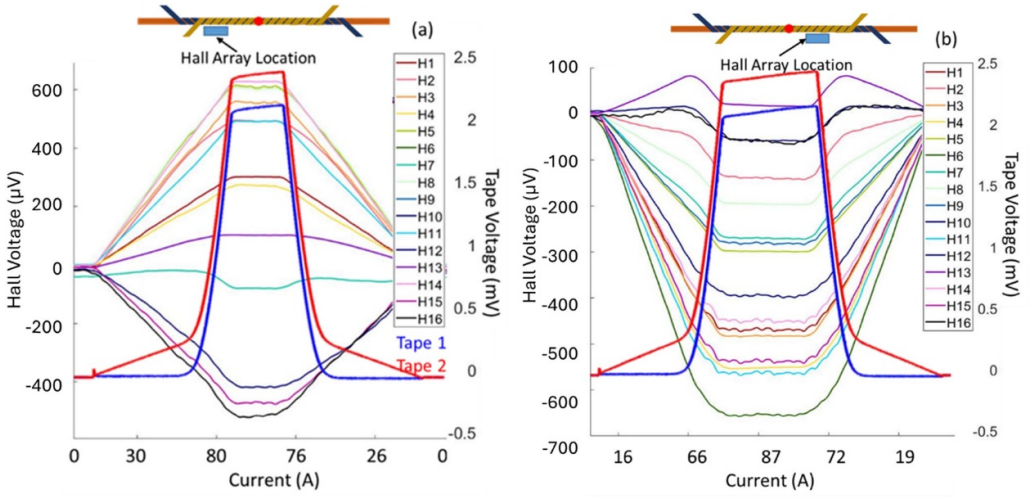

Figure 17. Hall response plotted against current (a) upstream of the defect, (b) downstream of defect.

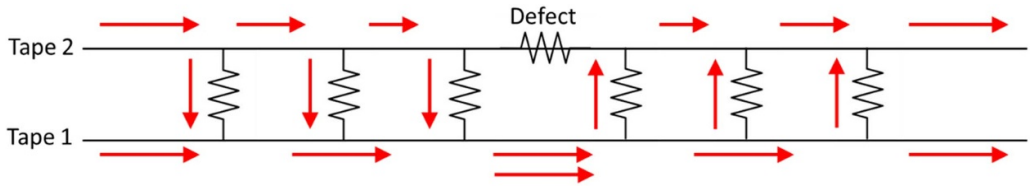

Figure 18. Simple circuit diagram showing interpreted current flow in the PbSn cable.

4.3. Soldered cable with 100% tear in tape 2

The decreased R_c in the soldered cable, 2.5 $\mu\Omega$ cm^2, facilitated good enough contact between tapes that there is no clear shift in the Hall signals along the cable. Instead, we see a large spread (500–800 μV) in Hall voltages along the entire length of the cable, figure 20. While there is no shift at the defect, we do see a trend of positive signals upstream and negative signals downstream. Figure 21 shows an example of what the Hall response looks like over the entire measurement cycle. Note that the voltages in both tapes remain stable while holding the cable current compared to the Ohmic rise observed in the PbSn and Cu cables, figures 12 and 16. When R_c is sufficiently small, more dynamic current sharing occurs. This permits the cable to better compensate for the defect. If the current is pushed farther above I_c perhaps the shift in Hall response might become evident in the soldered cable. However, it is not possible to push the current that high with the unwound ends, which would end up burning before the hotspot at the defect.

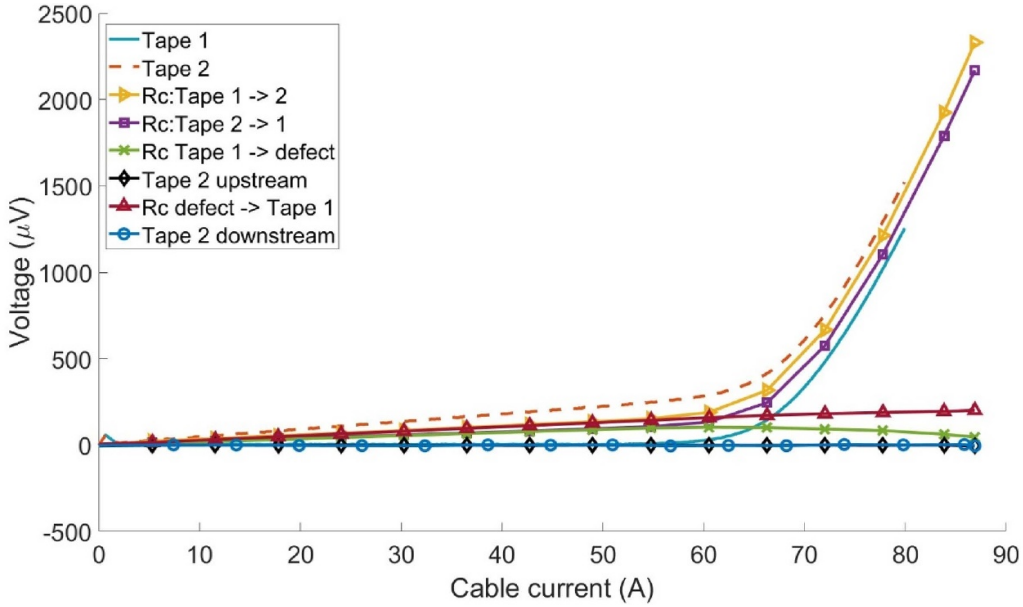

Figure 19. Voltages in the PbSn cable.

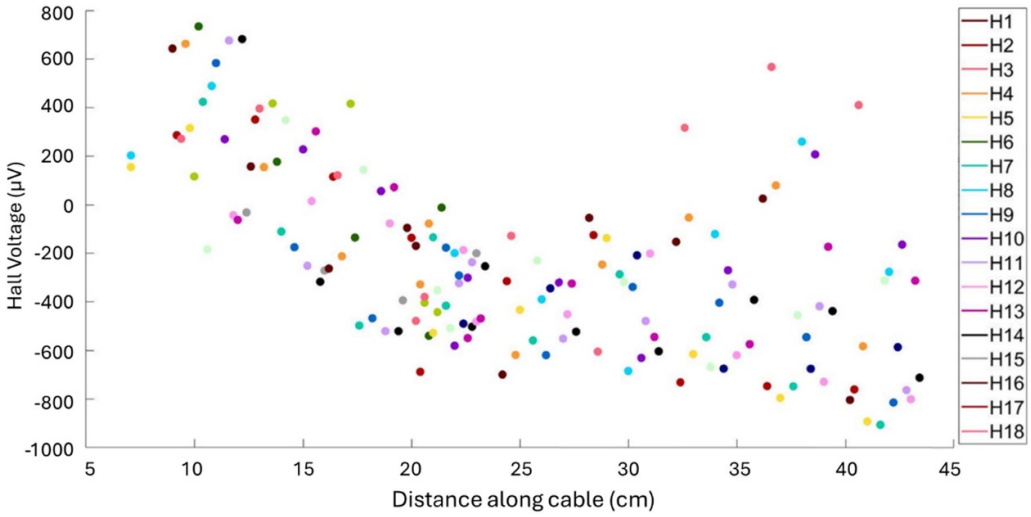

Figure 20. Hall Voltages along the length of the soldered cable.

The voltages in the soldered cable are an order of magnitude smaller than those in the PbSn cable and two orders smaller than in the Cu cable, figure 22. We also see some major differences in the soldered cable compared to the other two.

1. *The Normal zone spreads to Tape 2*. The Tape 2 section downstream (circles) has a resistive slope for the entire ramp and then begins to transition shortly after Tape 1 (solid line). The section upstream of the defect (diamonds) also begins to produce a small voltage, 15 μV at 75 A, which remains below the 1 μv cm^{-1} criterion.
2. *The normal zone is concentrated on the downstream side of the defect*. Again, we see this uneven voltage distribution around the defect. Since the downstream portion has more voltage it appears that the normal zone, or propagation of the hot spot, is concentrated downstream of the defect. This is potentially an artifact of the terminal resistance.

Melting the solder between tapes facilitates better current sharing within the cable, while also allowing a more even distribution of current injection. The effect of the R_t is greatly reduced as R_c is decreased. Figure 23 plots the current distribution in the cable, showing how Tape 2 now carries 42% of the current compared to only 16% in the Cu cable (figure 15).

5. Discussion

5.1. Cable performance

Current sharing is essential for cable stability and enhanced performance. Figure 21 shows that normal zones can persist

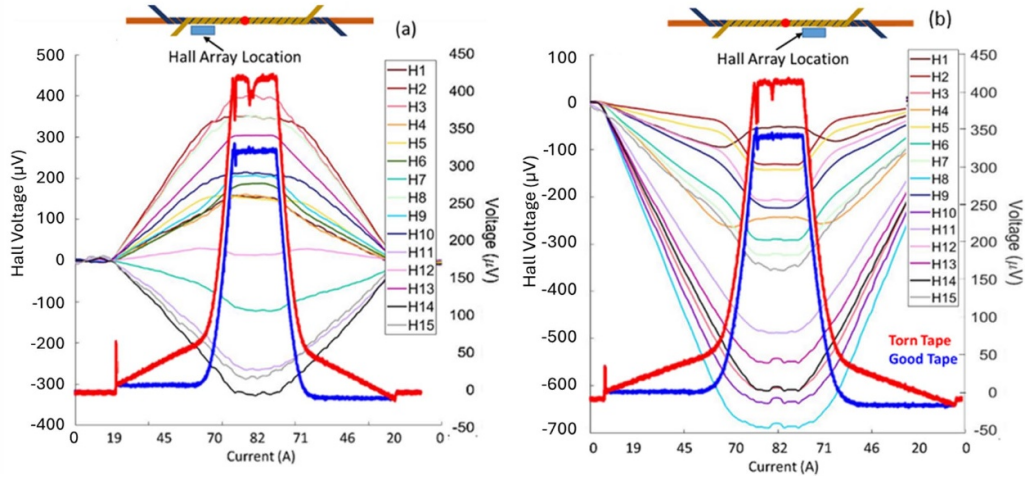

Figure 21. Hall voltages over entire current ramp (a) upstream of defect and (b) downstream of defect).

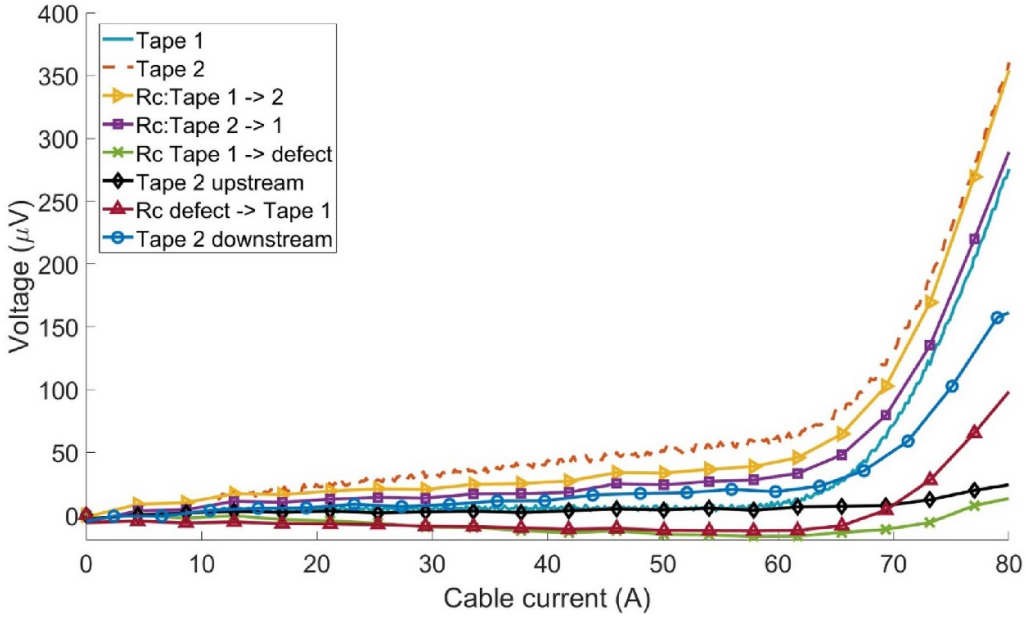

Figure 22. Voltages in Soldered cable.

even at currents well above I_c, and depending on R_c, significant dissipation can occur. Figure 24 plots of the V(I) transition in Tape 2, the torn tape, for the 3 cable types. At 60 A the Cu cable dissipates 590 mW, the PbSn cable dissipates 20 mW, and the soldered cable dissipates 5 mW. The majority of this dissipation occurs as current is transferred around the defect. These measurements were performed 20 times with no noticeable degradation. While cable performance remained stable during these experiments, one question we must ponder is: Does constant heating due to current transfer degrade contacts and how will it impact long term cable performance?

5.2. *Technique drawbacks etc*

One of the main drawbacks of this technique is that it is largely a qualitative approach. A shift in the polarity of the Hall voltages denotes the location of a severe defect in a simple 2 tape CORC® cable. However, this shift was only seen in cables with a large R_c relative to R_t. As R_c decreases it facilitates better sharing and the 'shift' in Hall voltages disappears. This shift is clearly evident in a 2-tape cable, but it is likely that as the number of tapes and layers increase so too will the difficulty of locating a defect. In general, a more significant drop in I_c corresponds to a more pronounced shift in signals, however the Hall sensors are unable to determine the severity of the defect.

On the other hand, improved position of the Hall array should improve the fidelity of signals. This device was our first attempt at developing a cable scanning system and there are many opportunities for refinement. Moreover, the experiments presented here have not been repeated in magnetic fields where inductive couplings come into play. Since the outer layer of the

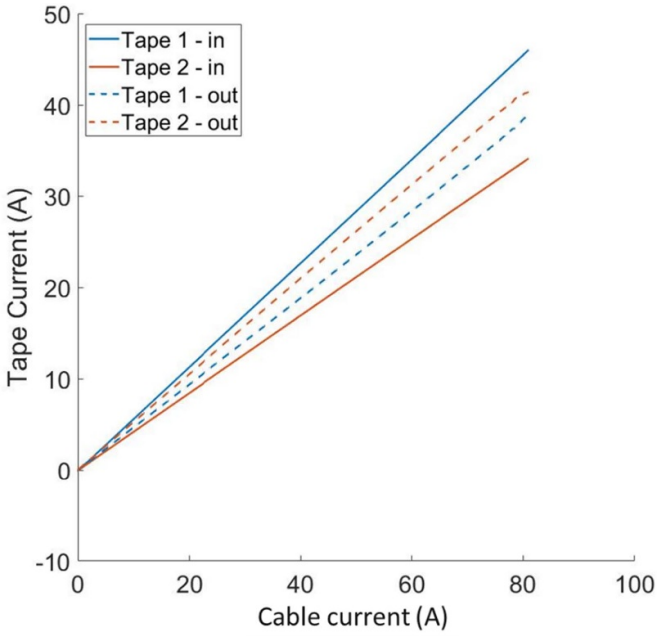

Figure 23. Current distribution in the soldered cable.

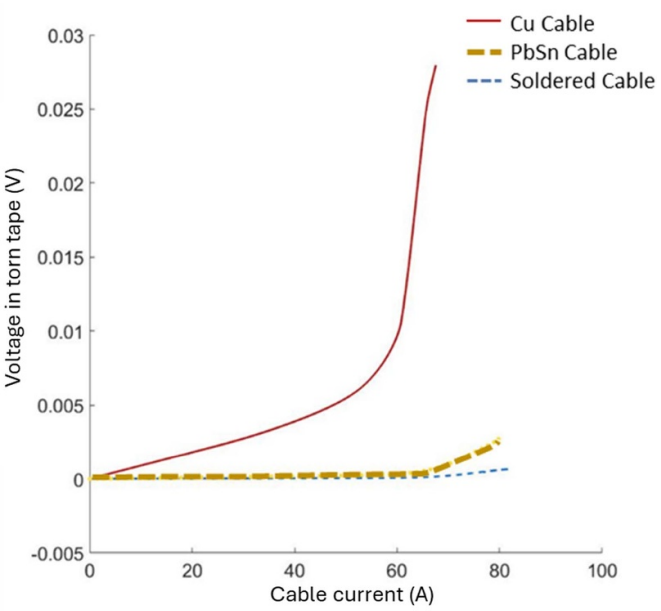

Figure 24. V(I) curve comparing the 3 different cables.

cable is the most vulnerable to damage from external sources and can only transfer current to one adjacent layer, scanned Hall probes could be especially sensitive to monitoring cable health.

5.3. Influence of terminations

A recent study looked at current sharing around defects in CORC® cables and how various parameters influence redistribution at the terminations as well as within the cable. Their simulations showed that even when cables contained conductors with local defects, the termination voltages forced a homogenous current distribution between conductors [15]. Another study looked into the balance between R_c and R_t in a stack of REBCO tapes and found that that $R_c \leqslant 0.4\ R_t$ in order to permit current sharing along the cable length rather than through the terminations [16].

In short cables, differing R_t can lead to non-uniform current distribution. Experiments and simulations have shown that the current will split according to R_t. Tapes with a smaller R_t will carry more current than conductors with a higher R_t. The current will distribute evenly between conductors as current increases near cable I_c [17, 18]. ACT has designed special cable terminations in order to prevent uneven current injection. The layers are tapered at the ends of the cable such that each layer comes into direct contact with the copper termination tube. The terminations are then filled with solder resulting in an R_t on the order of 100 nΩ [19]. However, in our experiments we wanted to measure the amount of current injected into each tape in the cable. Therefore, we unwound the tape ends and connected them to shunt resistors, creating a R_t several orders of magnitude larger than our R_c. Our large, and sometimes imbalanced R_t forced some current transfer in our cables and may have played a significant role in the current distribution between our conductors. This can have serious implications on power dissipation as it forces degraded tapes to carry excessive currents. This affect can be seen in the Cu cable, figure 10, where the large R_t forces the current to transfer back into Tape 2 downstream of the defect.

6. Conclusions

We set out in this work to investigate whether non-invasive use of Hall probes could be used to diagnose changes in current patterns in cables and locate where any defects or burnout spots may have resulted from cable testing. While the accuracy of identifying the location depends on the contact resistance and other factors, we clearly see signals correlated to locations of intentional defects made in our simple 2-tape cable, suggesting that there is promise in this method. Further demonstrations in magnetic fields and with cables having higher tape count should be conducted.

The main takeaways from this work are: (1) increased spread in Hall voltages correlates to regions with increased current transfer, (2) there is a shift in the polarity of the Hall sensors at the defect (positive voltage upstream, negative voltage downstream), and (3) depending on R_c, cables can dissipate a significant amount of power even though the normal zone is stable.

The current distribution around complete I_c dropouts was investigated using a scanning Hall array. Three, two-tape cables were constructed by ACT to probe the impact of R_c on current transfer and cable performance. The Hall array produced a periodic signal based on the sensor locations with respect to the tape pitch. In regions where the current is flowing in the REBCO, along the cable axis, the spread in signals is 150 μV. The spread in Hall voltages can increase by an order of magnitude in regions of active current transfer.

A clear shift in the Hall response occurs at the defect location: current transfer produces a positive Hall voltage upstream of the defect and a negative Hall voltage downstream. In the soldered cable the Hall voltages are positive upstream and negative downstream, yet the clear shift is no longer present. Instead we see a gradual trend from positive to negative along the length of the cable. While this shift is prominent in two tape cable, it may not be as evident in cables containing more tapes and layers.

A somewhat counter-intuitive result occurs for current transfer around a defect with high contact resistance. Voltage is developed in an adjacent 'pristine' conductor due to its overloaded state, which can lead to burnout of that conductor, when in fact the root cause is a flaw in an adjacent conductor. The apparent reluctance to transfer current in cables with high R_c to avoid such a burnout threat is also dependent on the length between defects and termination resistance. This could be especially problematic for the outer layer of the cable because the number of current sharing pathways is one-half that of the inner conductors. As R_c decreases this condition goes away as seen by the large spread in signals in figures 16 and 20.

Data availability statement

The data that support the findings of this study are openly available at the following URL/DOI: http://doi.org/10.6084/m9.figshare.26536282.

Acknowledgment

This work was completed at the Applied Superconductivity Center, which is a division within the National High Magnetic Field Laboratory, in Tallahassee, Fl. This work was supported by the National High Magnetic Field Laboratory, which is supported by National Science Foundation through DMR-218556 (this work was completed during the 2018-2022 grant NSF/DMR-1644779) and by the US Department of Energy under Grant Numbers DE-EE0007872, DE-SC0022011 and DE-SC0014009. We would like to acknowledge Griffin Bradford at the Applied Superconductivity Center for his technical support and Maxim Marchevsky and Reed Teyber at Lawrence Berkeley National Lab for their insight into current transfer in CORC®.

ORCID iDs

V Phifer 0000-0002-9755-8072
L Cooley 0000-0003-3488-2980
D van der Laan 0000-0001-5889-3751
J Weiss 0009-0009-2643-058X

References

[1] MacManus-Driscoll J and Wimbush S 2021 *Nat. Rev. Mater.* **6** 587–604
[2] Hu X *et al* 2016 *IEEE Trans. Appl. Supercond.* **27** 1–5
[3] Tsuchiya K *et al* 2017 *Cryogenics* **85** 1–7
[4] Nakasaki R *et al* 2015 *Int. Conf. on Magnet Technology* (*Seoul, South Korea*)
[5] Francis A, Abraimov D, Viouchkov Y, Su Y, Kametani F and Larbalestier D C 2020 *Supercond. Sci. Technol.* **33** 044011
[6] Miller D, Maroni V A, Hiller J M, Koritala R E, Chen Y, Black J L R and Selvamanickam V 2009 *IEEE Trans. Appl. Supercond.* **19** 3176–9
[7] Hartnett W, Ramirez J, Olson T E R, Hopp C T, Jewell M C, Knoll A R, Hazelton D W and Zhang Y 2021 *Eng. Res. Express* **3** 035007
[8] Weiss J, Mulder T, ten Kate H J and van der Laan D C 2017 *Supercond. Sci. Technol.* **30** 014002
[9] Wang X *et al* 2023 *IEEE Trans. Appl. Supercond.* **33** 4000608
[10] van der Laan D, Radcliff K, Anvar V A, Wang K, Nijhuis A and Weiss J D 2021 *Supercond. Sci. Technol.* **34** 10LT01
[11] Phifer V, Small M, Bradford G, Weiss J, van der Laan D and Cooley L 2022 *Supercond. Sci. Technol.* **35** 065003
[12] Warnes W 1987 *J. Appl. Phys.* **63** 1651
[13] Marchevsky M, Xie Y-Y and Selvamanickam V 2010 *Supercond. Sci. Technol.* **23** 034016
[14] Teyber R, Marchevsky M, Prestemon S, Weiss J and van der Laan D 2020 *Supercond. Sci. Technol.* **33** 095009
[15] Teyber R, Marchevsky M, Martinez A C A, Prestemon S, Weiss J and van der Laan D 2022 *Supercond. Sci. Technol.* **35** 094008
[16] Martinez A, Ji Q, Prestemon S O, Wang X and Maury Cuna G H I 2020 *IEEE Trans. Appl. Supercond.* **30** 6600605
[17] Pothavajhala V, Graber L, Han Kim C and Pamidi S 2014 *IEEE Trans. Appl. Supercond.* **24** 4800505
[18] Willering G, van der Laan D C, Weijers H W, Noyes P D, Miller G E and Viouchkov Y 2015 *Supercond. Sci. Technol.* **28** 035001
[19] Majoros M, D Sumption M, Collings E W and Long N J 2015 *Supercond. Sci. Technol.* **28** 055010
[20] Phifer V 2023 Experimental Investigations of Tape-to-Tape Contact Resistance and Its Impact on Current Distribution Around Local Ic Degradations in CORC® Cables Florida State University (available at: www.proquest.com/openview/90c3e2668a332c14b8cbcbefdb966763/1?pq-origsite=gscholar&cbl=18750&diss=y)